International Journal of Thermal Sciences 48 (2009) 1673–1678

Contents lists available at ScienceDirect

International Journal of Thermal Sciences

journal homepage: www.elsevier.com/locate/ijts

Slip-flow heat transfer in microtubes with axial conduction and viscous dissipation – An extended Graetz problem

Barbaros Çetin [a,*], Almila Gűvenç Yazicioğlu [b], Sadik Kakaç [c]

[a] Department of Mechanical Engineering, Vanderbilt University, Nashville, TN 37235, USA
[b] Department of Mechanical Engineering, Middle East Technical University, 06531 Ankara, Turkey
[c] Department of Mechanical Engineering, TOBB University of Economics and Technology, 06560 Ankara, Turkey

A R T I C L E I N F O

Article history:
Received 29 October 2008
Received in revised form
6 February 2009
Accepted 8 February 2009
Available online 17 March 2009

Keywords:
Microtube
Slip-flow
Heat transfer
Graetz problem

A B S T R A C T

This study is an extension of the Graetz problem to include the rarefaction effect, viscous dissipation term and axial conduction with constant-wall-heat-flux thermal boundary condition. The energy equation is solved analytically by using general eigenfunction expansion. The temperature distribution and the local Nusselt number are determined in terms of confluent hypergeometric functions. The effects of the rarefaction, axial conduction and viscous dissipation on the local Nusselt number are discussed in terms of dimensionless parameters such as the Knudsen number, Peclet number and Brinkman number.

1. Introduction

The Graetz problem, which is the problem of hydrodynamically-developed, thermally developing laminar flow of an incompressible fluid inside a tube neglecting the axial conduction and viscous dissipation, was solved analytically by Graetz [1,2] and Nusselt [3] more than a century ago. Many studies extended the Graetz problem to include additional effects (such as the axial conduction and viscous dissipation) and different channel geometries at the macroscale. An excellent review on the solution of the Graetz problem at the macroscale can be found elsewhere [4].

As the ratio of the mean-free-path (λ) to the characteristic length of the flow (L)–which is known as the Knudsen number ($Kn = \lambda/L$) – increases, the continuum approach fails to be valid, and the fluid modeling moves from continuum to molecular model. For the Kn number varying between 0.01 and 0.1 (which corresponds to the flow of the air at standard atmospheric conditions through the channel that has the characteristic length of 1–10 μm), the regime is known as the slip-flow regime and the continuum modeling together with the slip-velocity and the temperature-jump boundary conditions (the rarefaction effect) are valid [5]. More recently, the Graetz problem has also been extended to study the microscale flows by including the rarefaction effect both analytically [6–12] and numerically [13–15].

The characteristic lengths of the microchannels are very small, therefore viscous forces dominate inertial forces leading to a low Re (i.e. $Re \ll 1$) and a low Pe ($Pe = RePr$). For flows with a small Peclet number, the axial conduction term cannot be neglected, since the characteristic time of the convection and the diffusion becomes comparable, and the convection term no longer dominates the conduction term in the longitudinal direction. The Graetz problem with the inclusion of the axial conduction term has been an interesting problem due to the presence of the non self-adjoint eigenvalue problem. Accordingly, the linearly independent eigenfunctions become non-orthogonal [16]. This interesting problem has been studied by many researchers for macrochannels both analytically [17–26] and computationally [27,28] for more than three decades ago. More recently, Hadjiconstantinou and Simek [29] studied the effect of axial conduction for thermally fully-developed flows in micro and nano channels; and Jeong and Jeong [30] studied the effect of axial conduction together with viscous dissipation in slit channels with micro spacing for thermally developing flow. Çetin et al. [31] studied the same problem for a microtube numerically. Dutta et al. [32] and Horiuchi et al. [33] studied the thermal characteristics of mixed electroosmotic and pressure-driven microflows with the axial conduction.

This present study extends the Graetz problem to include the rarefaction effect, viscous dissipation term, and axial conduction in

* Corresponding author. Tel.: +1 615 343 9925; fax: +1 615 343 6687.
E-mail address: barbaros.cetin@vanderbilt.edu (B. Çetin).
URL: http://people.vanderbilt.edu/barbaros.cetin

1290-0729/$ – see front matter © 2009 Elsevier Masson SAS. All rights reserved.
doi:10.1016/j.ijthermalsci.2009.02.002

Nomenclature

A_m	coefficients of eigenfunctions
Br	Brinkman number ($\mu u_m^2/q_w R$)
C	matrix defined in Eq. (29)
D	matrix defined in Eq. (30)
F_m	eigenfunctions
FT	thermal accommodation factor
k	thermal conductivity
$\tilde{K}$	matrix defined in Eq. (10)
Kn	Knudsen number (λ/L)
$\tilde{L}$	matrix defined in Eq. (9)
$\tilde{N}$	matrix defined in Eq. (9)
$Nu_{\bar{x}}$	Local Nusselt number ($h_{\bar{x}}D/k$)
Pe	Peclet number ($RePr$)
Pr	Prandtl number (ν/α)
q_w	wall heat flux
r	radial coordinate
$\bar{r}$	non-dimensional radial coordinate
R	tube radius
Re	Reynolds number ($\rho u_m D/\mu$)
T	temperature
T_i	inlet temperature
u	velocity
$\bar{u}$	non-dimensional velocity
u_m	mean velocity
x	axial coordinate

Greek Letters

β_m	eigenvalues
γ	specific heat ratio
η	non-dimensional radial coordinate
θ	dimensionless temperature
θ_∞	fully-developed temperature
κ	parameter defined in Eq. (34)
λ	mean-free-path
μ	viscosity
ξ	non-dimensional axial coordinate
ρ_s	slip radius
ϕ	dimensionless temperature

the fluid for constant-wall-heat-flux boundary condition. By defining the appropriate non-dimensional parameters, the given problem is formulated in a similar form with its macroscale counterpart. The temperature distribution is determined analytically by using the general eigenfunction expansion and is obtained in terms of confluent hypergeometric functions. The effects of the rarefaction, axial conduction and viscous dissipation on the local Nu are discussed in terms of dimensionless parameters such as the Kn, Pe and Br.

2. Analysis

The steady-state, hydrodynamically-developed flow with a constant temperature, T_i, flows into the microtube with the constant heat flux at the wall, as shown in Fig. 1. By introducing the following dimensionless parameters,

$$\bar{r} = \frac{r}{R}, \quad \bar{x} = \frac{x}{PeR}, \quad \theta = \frac{T - T_i}{q_w R/k}, \quad \bar{u} = \frac{u}{u_m}, \quad Pe = RePr,$$
$$Br = \frac{\mu u_m^2}{q_w R}, \tag{1}$$

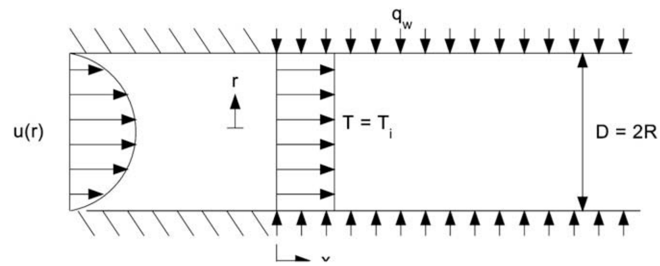

Fig. 1. Geometry of the problem.

the governing energy equation, including the axial conduction and the viscous dissipation term, and the corresponding boundary conditions can be written as [13]

$$\frac{\bar{u}}{2}\frac{\partial\theta}{\partial\bar{x}} = \frac{1}{\bar{r}}\frac{\partial}{\partial\bar{r}}\left(\bar{r}\frac{\partial\theta}{\partial\bar{r}}\right) + \frac{1}{Pe^2}\frac{\partial^2\theta}{\partial\bar{x}^2} + \frac{32Br}{(1+8Kn)^2}\bar{r}^2, \tag{2}$$

$$\theta = 0 \quad \text{at} \quad \bar{x} = 0, \tag{3}$$

$$\frac{\partial\theta}{\partial\bar{r}} = 0 \quad \text{at} \quad \bar{r} = 0, \tag{4}$$

$$\frac{\partial\theta}{\partial\bar{r}} = 1 \quad \text{at} \quad \bar{r} = 1, \tag{5}$$

$$\theta \to \theta_\infty \quad \text{at} \quad \bar{x} \to \infty, \tag{6}$$

where $\bar{u}$ is the dimensionless fully-developed velocity profile for the slip-flow regime defined as [31],

$$\bar{u} = \frac{2(1 - \bar{r}^2 + 4Kn)}{1 + 8Kn}, \tag{7}$$

and θ_∞ is the dimensionless fully-developed temperature profile which can be determined by applying the similar procedure to that for a macrochannel flow [34], and the solution can be written in matrix form as,

$$\tilde{M} = \begin{bmatrix} 1/4 & -1 & 7/24 & -4 & -8 \\ 2 & -4 & 1 & 16 & 32 \\ 3 & -14 & 14 & -64 & -128 \\ 18 & -36 & 11 & 192 & -384 \\ 18 & -108 & 41 & -576 & -1152 \\ 3 & -6 & 2 & 48 & -96 \\ 0 & 2 & -1 & 16 & 32 \\ 3 & -30 & 13 & -192 & -384 \end{bmatrix} \tag{8}$$

$$\tilde{N} = \begin{bmatrix} \bar{r}^4 \\ \bar{r}^2 \\ 1 \\ \bar{x} \\ 1/Pe^2 \end{bmatrix}, \quad \tilde{L} = -\frac{1}{(1+8Kn)^4}\begin{bmatrix} 1 \\ 2Br \\ 2Kn \\ 8BrKn \\ 8/3Kn^2 \\ 128/3BrKn^2 \\ -1024Kn^4 \\ 128/3Kn^3 \end{bmatrix} \tag{9}$$

$$\tilde{K} = \tilde{L}\left(\tilde{M}\tilde{N}\right), \tag{10}$$

$$\theta_\infty = \sum_{i=1}^{9}\tilde{K}_i. \tag{11}$$

When $Kn = Br = 0$, the solution recovers the macrochannel result [24] as,

$$\theta_\infty = 4\bar{x} + \bar{r}^2 - \frac{\bar{r}^4}{4} - \frac{7}{24} + \frac{8}{Pe^2}, \quad (12)$$

The solution to the energy equation, Eq. (2) can be assumed to be the superposition of two solutions as,

$$\theta(\bar{r},\bar{x}) = \phi(\bar{r},\bar{x}) + \theta_\infty(\bar{r},\bar{x}), \quad (13)$$

in which case the equation associated with $\phi(\bar{r},\bar{x})$ becomes homogeneous in the $\bar{r}$ direction, and can be further arranged by defining the following dimensionless parameters,

$$\eta = \bar{r}\rho_s, \quad \xi = \rho_s^2\left(2-\rho_s^2\right)x, \quad \tilde{P}e = \frac{Pe}{\rho_s^2\left(2-\rho_s^2\right)},$$
$$\rho_s^2 = \frac{1}{1+4Kn}, \quad (14)$$

where the ρ_s is the slip radius defined by Larrode et al. [8]. It takes into account the rarefaction effect. By introducing these variables, the equation and the boundary conditions associated with $\phi(\bar{r},\bar{x})$ can be written as follows,

$$\left(1-\eta^2\right)\frac{\partial\phi}{\partial\xi} = \frac{1}{\eta}\frac{\partial}{\partial\eta}\left(\eta\frac{\partial\phi}{\partial\eta}\right) + \frac{1}{\tilde{P}e^2}\frac{\partial^2\phi}{\partial\eta^2}, \quad (15)$$

$$\phi(\eta,0) = \theta_\infty\left(\frac{\eta}{\rho_s},0\right) \quad \text{at} \quad \xi = 0, \quad (16)$$

$$\frac{\partial\phi}{\partial\eta} = 0 \quad \text{at} \quad \eta = 0, \quad (17)$$

$$\frac{\partial\phi}{\partial\eta} = 0 \quad \text{at} \quad \eta = \rho_s, \quad (18)$$

$$\phi \to 0 \quad \text{at} \quad \xi \to \infty. \quad (19)$$

Eq. (15) has the same form as its macroscopic counterpart (i.e. macrotube flow without the viscous dissipation). The only difference is the boundary conditions (16) and (18). Setting $Br = 0$ and $Kn = 0$ would end up with exactly the same problem for the macrochannel flow. The macrochannel flow with low Pe was solved for both constant wall temperature [25] and constant-wall-heat-flux [24] boundary conditions. Therefore, the solution procedure of [24] will be extended to take into account the rarefaction and the viscous dissipation effects. Actually, the viscous dissipation term has already been included as the additional terms in the fully-developed temperature profile, Eq. (12).

We can assume the solution of $\phi(\eta,\xi)$ in the form of,

$$\phi(\eta,\xi) = \sum_{m=1}^{\infty} A_m F_m(\eta) e^{-\beta_m^2\xi}. \quad (20)$$

Introducing this solution into Eq. (15), it can be shown that the functions $F_m(\eta)$ and the eigenvalues β_m satisfy the following eigenvalue problem,

$$\frac{d}{d\eta}\left(\eta\frac{dF_m}{d\eta}\right) + \eta\beta_m^2\left(\frac{\beta_m^2}{\tilde{P}e^2} + 1 - \eta^2\right)F_m(\eta) = 0, \quad (21)$$

$$\frac{dF_m}{d\eta} = 0 \quad \text{at} \quad \eta = 0, \quad \frac{dF_m}{d\eta} = 0 \quad \text{at} \quad \eta = \rho_s. \quad (22)$$

Table 1
Comparison of the Local Nus from the present study with the available results from the literature ($pe \to \infty$).

ξ	$Kn = 0$		$Kn = 0.04$		$Kn = 0.08$	
	Present study	[23]	Present study	[12]	Present study	[12]
0.001	15.813	15.811	9.089	–	5.855	–
0.002	12.538	12.537	8.011	–	5.426	–
0.004	9.986	9.986	6.961	7.186	4.956	5.084
0.008	8.020	8.020	5.994	6.079	4.473	4.544
0.010	7.494	7.494	5.708	–	4.320	–
0.015	6.656	6.656	5.228	–	4.0521	–
0.020	6.148	6.148	4.920	4.950	3.874	3.916
0.040	5.198	5.198	4.312	4.329	3.504	3.534
0.080	4.621	4.621	3.923	3.931	3.260	3.276
0.100	4.514	4.514	3.849	3.855	3.215	3.226
0.200	4.375	4.375	3.756	3.757	3.159	3.161
0.400	4.364	4.364	3.749	3.749	3.156	3.155
1.000	4.364	4.364	3.749	3.749	3.156	3.155

Clearly, Eq. (21) does not belong to the usual Sturm–Liouville system. However, it can be shown that the functions $F_m(\eta)$ satisfy the following relation [24], which will be used during the determination of the coefficients A_m's,

$$\int_0^{\rho_s} \eta\left(\frac{\beta_m^2+\beta_n^2}{\tilde{P}e^2} + 1 - \eta^2\right)F_m(\eta)F_n(\eta)d\eta$$
$$= \begin{cases} 0 & \text{for} \quad m \neq n \\ N(\beta_m) & \text{for} \quad m = n \end{cases} \quad (23)$$

where,

$$N(\beta_m) = \int_0^{\rho_s} \eta\left(\frac{2\beta_m^2}{\tilde{P}e^2} + 1 - \eta^2\right)F_m^2(\eta)d\eta. \quad (24)$$

The solution to Eq. (21) can be expressed as,

$$F_m(\eta) = {}_1F_1(a;b;z)e^{-\beta_m\eta^2/2}, \quad (25)$$

where ${}_1F_1(a;b;z)$ is the confluent hypergeometric function (detailed information about hypergeometric functions can be found elsewhere [35]), and the arguments are given as,

$$a = \frac{1}{2} - \frac{\beta_m}{4}\left(\frac{\beta_m^2}{\tilde{P}e^2} + 1\right), \quad b = 1, \quad z = \beta_m\eta^2, \quad (26)$$

The eigenvalues can be determined by using the wall boundary condition, and the summation constants can be evaluated by using the inlet boundary condition. Note that eigenfunctions $F_m(\eta)$ are not mutually orthogonal (by referring to the standard Sturm–Liouville problem) since the eigenvalues occur non-linearly. To determine the coefficients A_m, similar procedure to that of Davis [26] is implemented. By using the inlet boundary condition, Eq. (27), the following relation can be obtained by truncating the series,

$$\sum_{m=0}^{N} A_m F_m(\eta) = -\theta_\infty\left(\frac{\eta}{\rho_s},0\right), \quad (27)$$

To determine A_m, we operate on Eq. (27) with the following operator,

$$\int_0^{\rho_s} \eta\left(\frac{\beta_n^2}{\tilde{P}e^2} + 1 - \eta^2\right)F_n(\eta)d\eta, \quad n = 1\ldots N \quad (28)$$

If our system was a standard Sturm–Liouville system, the resulting systems of equations would give a diagonal coefficient matrix. In

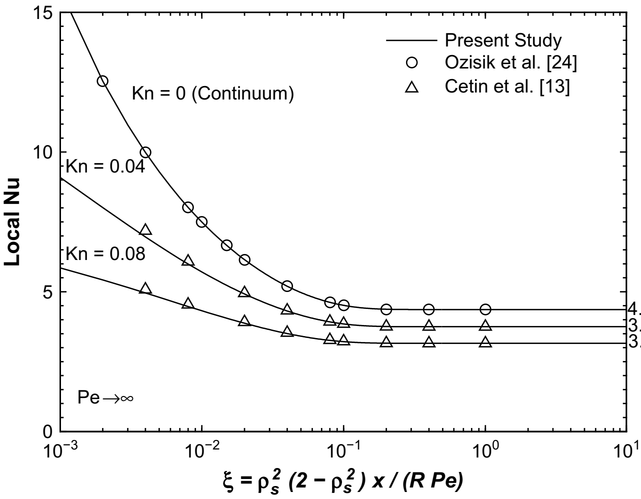

Fig. 2. Variation of the local Nu as a function of dimensionless axial coordinate for different Kn ($pe \to \infty$, $Br = 0$).

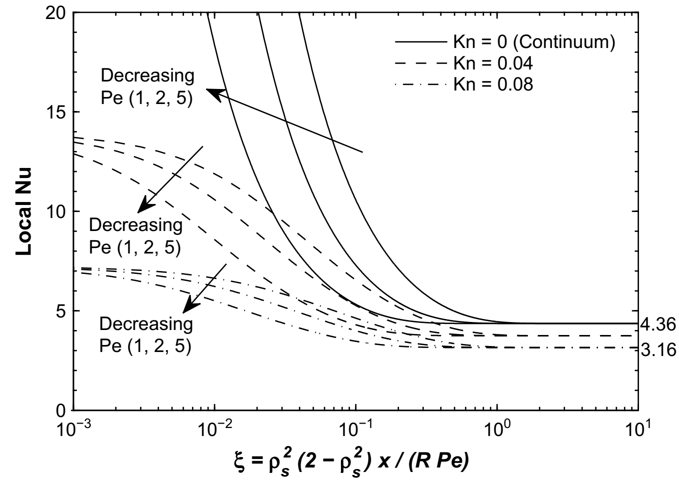

Fig. 3. Variation of the local Nu as a function of dimensionless axial coordinate for different Kn and Pe ($Br = 0$).

this case, the coefficient matrix is a full-matrix. The elements of the coefficient matrix are calculated by evaluating the corresponding integrals by using numerical integration. During the implementation, it has been observed that implementation of the relation defined by Eq. (23) for the calculation of the non-diagonal elements resulted in more efficient computation. The resulting algebraic system can be written as,

$$C_{m,n} = \begin{cases} -\displaystyle\int_0^{\rho_s} \eta \frac{\beta_n^2}{\tilde{P}e^2} F_m(\eta) F_n(\eta)\, \mathrm{d}\eta & \text{for} \quad m \neq n \\ N(\beta_m) & \text{for} \quad m = n \end{cases} \tag{29}$$

$$D_n = -\int_0^{\rho_s} \eta \left(\frac{\beta_n^2}{\tilde{P}e^2} + 1 - \eta^2 \right) F_n(\eta) \theta_\infty \left(\frac{\eta}{\rho_s}, 0 \right) \mathrm{d}\eta, \tag{30}$$

$$A_m = C_{mn}^{-1} D_n, \quad m = 1 \ldots N. \tag{31}$$

Once the eigenvalues, eigenfunctions and the coefficients A_m's are determined, the temperature field, $\theta(\bar{r}, \bar{x})$, can be determined. Knowing the temperature field and the temperature-jump boundary condition,

$$T - T_{wall} = \frac{2 - F_T}{F_T} \frac{2\gamma}{\gamma + 1} \frac{\lambda}{Pr} \left(\frac{\partial T}{\partial r} \right)_{r=R}, \tag{32}$$

the local Nu can be determined from,

$$Nu_{\bar{x}} = \frac{D}{T_{mean} - T_{wall}} \left(\frac{\partial T}{\partial r} \right)_{r=R} = -\frac{2}{\theta(1, \bar{x}) - \theta_{mean}(\bar{x}) - 2\kappa Kn}, \tag{33}$$

where κ is the dimensionless parameter defined as,

$$\kappa = \frac{2 - F_T}{F_T} \frac{2\gamma}{\gamma + 1} \frac{1}{Pr}, \tag{34}$$

where F_T is the thermal accommodation factor, γ is the specific heat ratio, and Pr is the Prandtl number of the fluid. θ_{mean} is the dimensionless mean temperature defined as,

$$\theta_{mean}(\bar{r}) = 2 \int_0^1 \bar{u} \theta(\bar{r}, \bar{x}) \bar{r} \mathrm{d}\bar{r}. \tag{35}$$

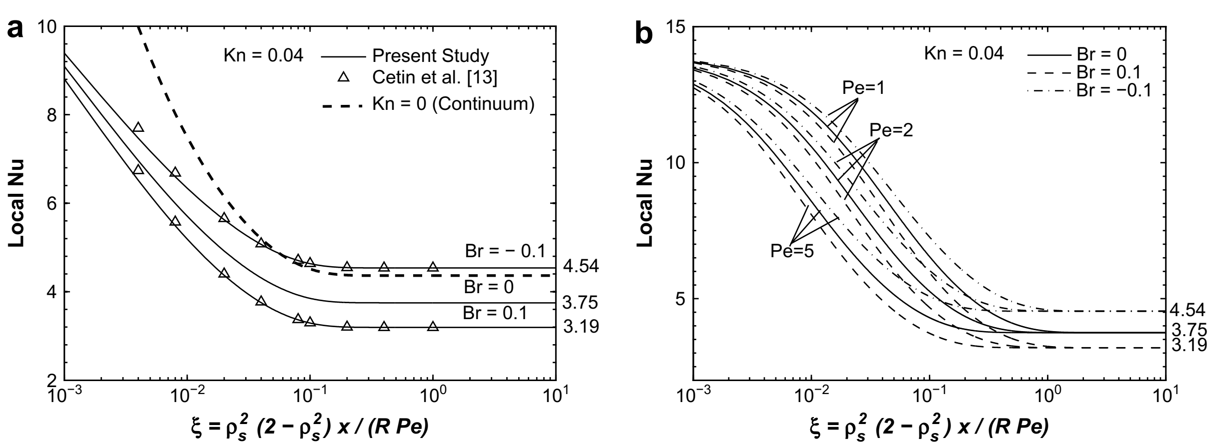

Fig. 4. Variation of the local Nu as a function of dimensionless axial coordinate for different Br ($Kn = 0.04$) (a) $pe \to \infty$, (b) low Pe.

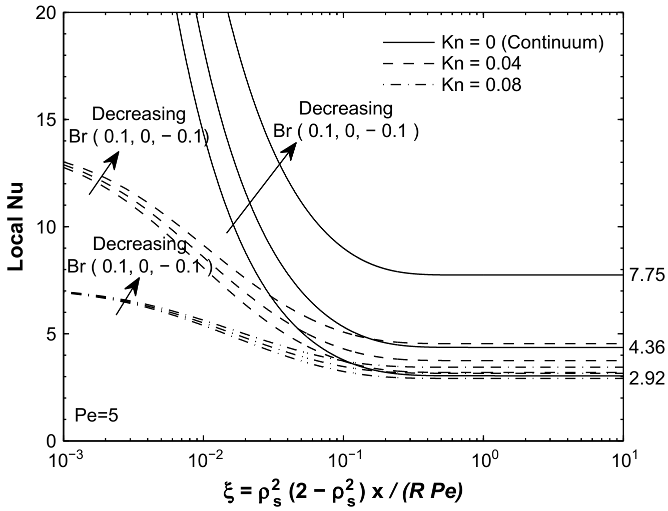

Fig. 5. Variation of the local *Nu* as a function of dimensionless axial coordinate for different *Br* and *Kn* ($Pe = 5$).

3. Results and discussions

The heat transfer characteristics of the extended Graetz problem is analyzed by solving the governing equation, Eq. (2), by using superposition and the general eigenfunction expansion. The procedure described in the former section is coded by the help of the *Mathematica*® software. The eigenvalues are obtained by using the built-in function *FindRoot* and the numerical integrations are performed by use of the built-in function *NIntegrate*. $N = 20$ eigenvalues are used in the evaluation of the temperature distribution.

Kn is varied between 0 and 0.1 which are the applicability limits of the slip-flow regime. Parameter κ is taken as 1.667 which is a typical value for air – the working fluid in many engineering applications. *Pe* is varied between 1 and 5, and it is taken as 10^6 to demonstrate $Pe \to \infty$ case. Present results are compared with the available results in the literature. The comparison of the results for $Pe \to \infty$ (i.e. without axial conduction) and $Br = 0$ (i.e. no viscous dissipation) are tabulated in Table 1 and also plotted in Fig. 2 for different *Kn*. As seen from the table and the graph, a good agreement has been achieved with 20 eigenvalues.

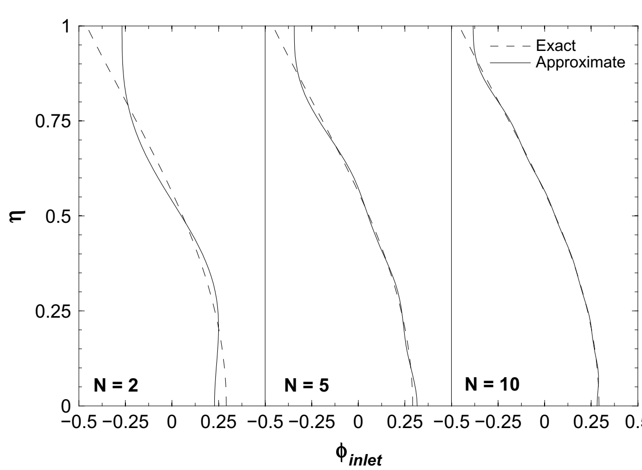

Fig. 6. Comparison of the RHS and LHS of Eq. (27) for different number of eigenfunctions.

In Fig. 3, the variation of the local *Nu* is plotted for different *Kn* for low *Pe*. By the inclusion of the rarefaction, the gradient at the wall tends to decrease because of the temperature-jump at the wall which leads to a decrease of the local *Nu*. Therefore, the increase in *Kn* results in lower *Nu*. As *Pe* increases, the thermal entrance length (i.e. the point where the local *Nu* reaches its asymptotic value) increases due to the effect of the axial conduction. Keeping in mind that our *x*-axis is non-dimensional, the difference in the thermal entrance length would be less pronounced in the dimensional case.

Fig. 4 illustrates the variation of the local *Nu* along the channel for different *Kn*, and for $Pe \to \infty$ (Fig. 4(a)), and for low *Pe* (Fig. 4(b)). Results of Çetin et al. [13] are also included in Fig. 4(a), and the results show a good agreement. Positive *Br* means that the fluid is being heated and negative *Br* means that the fluid is being cooled. Since the viscous dissipation is the result of the velocity gradient, it is more pronounced near the wall where the velocity gradient is significant. Therefore, the viscous dissipation affects the surface temperature more significantly than the mean temperature [4]. As a result, the difference between the wall temperature and the mean temperature increases with increasing *Br* and leads to a lower local *Nu*. For the $Br < 0$ case, the situation is vice-versa and leads to a higher local *Nu*. Again, as *Pe* decreases, the entrance length increases.

Fig. 5 shows the variation of the local *Nu* for different *Br* and *Kn*. The difference between different *Br* is more significant for the $Kn = 0$ case, and less pronounced as rarefaction increases. By the introduction of the rarefaction, the velocity profile loses its steepness because of the presence of the slip-velocity, especially near the wall. Therefore, the effect of the viscous dissipation becomes less significant and deviation from the $Br = 0$ case diminishes.

Although the general eigenfunction expansion is a well-developed method, the completeness of the eigenfunctions is a critical issue for the convergence of the solution. For the standard Sturm–Liouville system, the completeness of the eigenfunctions is inherently satisfied. However, for our system, the completeness of the eigenfunctions is questionable. Some previous studies [24,25] also mentioned this issue, and assumed completeness by comparing the accuracy of their results with other studies instead of a rigorous mathematical proof. In this study, the convergence of the solution is checked by comparing the RHS and LHS of the Eq. (27) with increasing number of eigenfunctions. Fig. 6 shows the LHS and RHS of the Eq. (27) for different number of eigenfunctions. As seen from the figure, the convergence is clear for increasing *N*. There is a deviation near the wall due to singularity at the corner of the inlet. Referring to this graph, we can conclude that our eigenfunction expansion converges. $N = 20$ is taken in this study for better accuracy.

4. Conclusions

In this study, the Graetz problem is revisited to include the rarefaction effect, the viscous dissipation term, and the axial conduction in the fluid for the constant-wall-heat-flux boundary condition to analyze the heat transfer characteristics of the fluid flow inside a microtube. The energy equation is solved by using general eigenfunction expansion by the help of the *Mathematica*®. The effects of the *Kn*, *Pe* and *Br* on the local *Nu* are discussed. It is found that the local *Nu* decreases with increasing *Kn* and *Br*. The local *Nu* converges to the same fully-developed *Nu* for different *Pe*, and the thermal entrance length increases with decreasing *Pe*. The effect of *Br* on the local *Nu* is found to be less pronounced as the rarefaction increases (i.e. increasing *Kn*).

Acknowledgments

Financial support from the Turkish Scientific and Technical Research Council, Grant No. 106M076, is greatly appreciated. Mr Çetin would like to thank the Ezici family for their continuous support during the preparation of the manuscript.

References

[1] L. Graetz, Uben die wärmeleitungsfähigkeit von flüssigkeiten. (On the thermal conductivity of liquids, part 1), Ann. Phys. Chem. 18 (1883) 79–94.
[2] L. Graetz, Uben die wärmeleitungsfähigkeit von flüssigkeiten. (On the thermal conductivity of liquids, part 2), Ann. Phys. Chem. 25 (1885) 337–357.
[3] W. Nusselt, Die abhängigkeit der wärmeübergangszahl von der rohrlänge. (The dependence of the heat transfer coefficient on the tube length), VDI Z 54 (1910) 1154–1158.
[4] A.L.R.K. Shah, Laminar Flow Forced Convection in Ducts: A Source Book for Compact Heat Exchanger Analytical Data, Academic Press, 1978, pp. 78–138.
[5] Y. Yener, S. Kakac, M. Avelino, T. Okutucu, Single phase forced convection in microchannels- state-of art-review, Microscale Heat Transfer-Fundamentals and Applications in Biological Systems and MEMS, Kluwer Academic Publisher, 2005, 1–25.
[6] T.A. Ameel, R.F. Barron, X.M. Wang, R.O. Warrington, Heat transfer in microtubes with viscous dissipation, Int. J. Heat Mass Transfer 44 (2001) 2395–2403.
[7] G. Tunc, Y. Bayazitoglu, Convection at the entrance of micropipes with sudden wall temperature change, in: ASME IMECE 2002, November 17–22, 2002, New Orleans, Louisiana.
[8] F.E. Larrode, C. Housiadas, Y. Drossinos, Slip-flow heat transfer in circular tubes, Int. J. Heat Mass Transfer 43 (2000) 2669–2680.
[9] M.D. Mikhailov, R.M. Cotta, S. Kakac, Steady state and periodic heat transfer in micro conduits, Microscale Heat Transfer-Fundamentals and Applications in Biological Systems and MEMS, Kluwer Academic Publisher, 2005.
[10] R.F. Barron, X.M. Wang, R.O. Warrington, T.A. Ameel, The Graetz problem extended to slip flow, Int. J. Heat Mass Transfer 40 (1997) 1817–1823.
[11] T.A. Ameel, R.F. Barron, X.M. Wang, R.O. Warrington, Laminar forced convection in a circular tube with constant heat flux and slip flow, Microscale Therm. Eng. 1 (1997) 303–320.
[12] S.B. Choi, R.F. Barron, R.O. Warrington, Fluid flow and heat transfer in microtubes, micromechanical sensors, actuators, and systems, ASME DSC 32 (1991) 123–134.
[13] B. Çetin, H. Yuncu, S. Kakac, Gaseous flow in microchannels with viscous dissipation, Int. J. Transport Phenom. 8 (2006) 297–315.
[14] H.P. Kavehpour, M. Faghri, Y. Asako, Effects of compressibility and rarefaction in gaseous flows in microchannels, Numer. Heat Tran. 32 (1997) 677–696.
[15] B. Xu, K.T. Ooi, C. Mavriplis, M.E. Zaghloul, Evaluation of viscous dissipation in liquid flow in microchannels, J. Micromechi. Microeng. 13 (2003) 53–57.
[16] W.M. Deen, Analysis of Transport Phenomena, Oxford University Press, 1998, pp. 391–392.
[17] R.L. Ash, J.H. Heinbockel, Note on heat transfer in laminar fully developed pipe flow with axial conduction, Math. Phys. 21 (1970) 266–269.
[18] C.J. Hsu, An exact analysis of low Peclet number thermal entry region heat transfer in transversely non-uniform velocity field, AIChE J. 17 (1971) 732–740.
[19] V. Taitel, A. Tamir, Application of the integral method to flows with axial conduction, Int. J. Heat Mass Transfer 15 (1972) 733–740.
[20] V. Taitel, M. Bentwich, A. Tamir, Effects of upstream and downstream boundary conditions on heat (mass) transfer with axial diffussion, Int. J. Heat Mass Transfer 16 (1973) 359–369.
[21] E. Papoutsakis, D. Ramkrishna, H.C. Lim, The extended Graetz problem with Dirichlet wall boundary condition, Appl. Sci. Res. 36 (1980) 13–34.
[22] E. Papoutsakis, D. Ramkrishna, H.C. Lim, The extended Graetz problem with prescribed wall flux, AIChE J. 26 (1980) 779–787.
[23] A. Acrivos, The extended Graetz problem at low Peclet numbers, Appl. Sci. Res. 36 (1980) 35–40.
[24] B. Vick, M.N. Ozisik, An exact analysis of low Peclet number heat transfer in laminar flow with axial conduction, Lett. in Heat Mass Transfer 8 (1981) 1–10.
[25] J. Lahjomri, A. Qubarra, Analytical solution of the Graetz problem with axial conduction, J. Heat Transfer 121 (1999) 1078–1083.
[26] E. Davis, Exact solutions for a class of heat and mass transfer problems, Can. J. Chem. Eng. 51 (1971) 562–572.
[27] F.H. Verhoff, D.P. Fisher, A numerical solution of the Graetz problem with axial conduction, J. Heat Transfer 95 (1973) 124–132.
[28] M.L. Michelsen, J. Villadsen, The Graetz problem with axial heat conduction, Int. J. Heat Mass Transfer 17 (1974) 1391–1402.
[29] N.G. Hadjiconstantinou, O. Simek, Constant-wall-temperature Nusselt number in micro and nano-channels, J. Heat Transfer 124 (2002) 356–364.
[30] H.E. Jeong, J.T. Jeong, Extended Graetz problem including streamwise conduction and viscous dissipation in microchannels, Int. J. Heat Mass Transfer 49 (2006) 2151–2157.
[31] B. Çetin, A. Yazicioglu, S. Kakac, Fluid flow in microtubes with axial conduction including rarefaction and viscous dissipation, Int. Comm. Heat Mass Transfer 35 (2008) 535–544.
[32] P. Dutta, K. Horiuchi, H.M. Yin, Thermal characteristics of mixed electroosmotic and pressure-driven microflows, Comput. Math. Appl. 52 (2006) 651–670.
[33] K. Horiuchi, P. Dutta, A. Hossain, Joule-heating effects in mixed electroosmotic and pressure-driven microflows under constant wall heat flux, J. Eng. Math. 54 (2006) 159–180.
[34] L. Leal, Advanced Transport Phenomena: Fluid Mechanics and Convective Transport Processes, Cambridge University Press, 1995, pp. 468–469.
[35] G. Arfken, H. Weber, Mathematical Methods For Physicists, Academic Press, 2005, pp. 796–799.